

THE USE OF ELECTROPOLISHING SURFACE TREATMENT ON IN718 PARTS FABRICATED BY LASER POWDER BED FUSION PROCESS

Li Yang^{*}, Chris O'Neil[†], Yan Wu^{*}

^{*}Department of Industrial Engineering, University of Louisville

[†]Department of Mechanical Engineering, University of Louisville

Abstract

In various applications of additively manufactured Ni-based superalloys, high surface finish quality is required. In this work, electropolishing surface treatment with anhydrous electrolyte solution was employed to improve the surface quality of the IN718 parts fabricated by laser powder bed fusion process. Various process parameters including electropolishing voltage, temperature, electrolyte spacing and electrolyte flow speed were investigated for their effect on the improvement of surface roughness characteristics. In addition, the effect of electrolyte flow uniformity on the surface quality deviation was investigated. The results provided additional insights to the recently proposed polishing methods proposed by the same group, which clearly indicates the potential benefit of introducing highly regulated electrolyte flow in the polishing of AM metal parts.

Keywords: Electropolishing, surface treatment, powder bed fusion, superalloy, IN718, additive manufacturing

Introduction

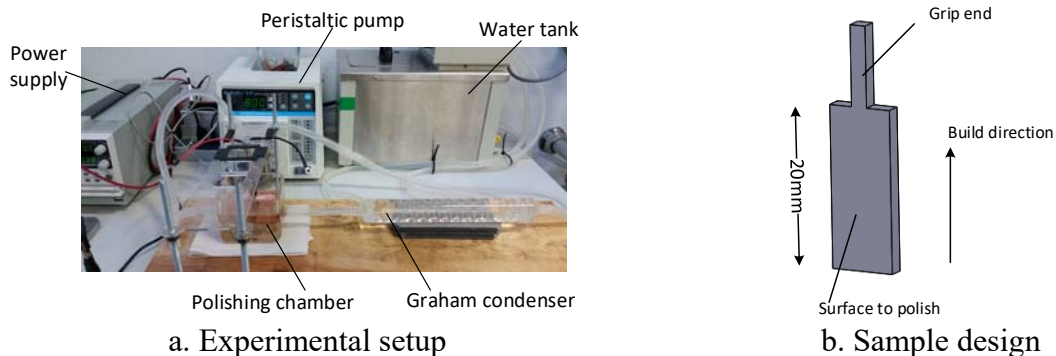
Ni-based superalloys are widely used in aerospace applications for components subjected to high operation temperatures such as the turbine engines [1-3]. Mainly employed as precipitation hardening alloys, the Inconel 718 (IN718) alloy exhibit good high-temperature strength, high toughness, high corrosion resistance, high wear resistances, good impact response, and very good weldability, which makes it attractive for applications [1-7]. However, due to its exceptional mechanical properties, IN718 also exhibits very low machinability, which makes it very challenging for the traditional manufacturing processes to create high quality components [2, 4, 8-10]. In recent years, the use of powder bed fusion additive manufacturing (PBF-AM) for the direct fabrication of IN718 parts has been successfully demonstrated [11-14]. As an additive manufacturing (AM) technology, PBF-AM possesses promising potentials in the fabrication of IN718 structures, such as freeform geometry capabilities, good control of microstructures and precipitates, short lead time and less material wastes. However, it is widely recognized that the surface quality of the structures fabricated by PBF-AM tend to be rough, which is contributed by both the staircase effect typical to AM processes as well as the process characteristics of PBF-AM. The surface finish of the PBF-AM is strongly influenced by both the powder feedstock characteristics and the process parameters [15-17]. Due to the highly transient melting pool dynamics during the melting and solidification, the boundaries of the PBF-AM solid materials often exhibit large degree of irregularity, which is further signified by the partial sintering/melting of the powder particle on the surfaces [18, 19]. Although in-process parameter optimization could partially offset such issues, due to the intrinsic randomness with the powder feedstock characteristics, the surface qualities of the PBF-AM processes is likely limited [17, 20]. On the other hand, for many aerospace applications high surface quality is required for structural

components in order to ensure satisfactory fatigue and corrosion resistance performance, therefore, for many IN718 components fabricated by PBF-AM additional post-treatment is needed to improve the surface qualities.

Due to the high mechanical properties of IN718, machining based surface treatment is difficult, and the good corrosion resistance of IN718 also makes it difficult for well-controlled chemical etching based polishing [21, 22]. The use of electropolishing for the surface treatment of nickel and IN718 alloys has been previously reported using various recipes [21, 23, 24]. In addition, as the surface oxidation mechanism of the IN718 exhibits similar electropolishing effect to the Ti-alloys, additional literatures can be found with the electropolishing of Ti-alloys and NiTi alloys, which provide additional information about recipe options [25-28]. In our previous studies, we used a non-aqueous alcoholic solution for the electropolishing of Ti6Al4V fabricated by electron beam melting, which was believed to have various advantages over the other electrolyte such as low toxicity and lack of oxidation layer formation [29, 30]. In the current study, we investigate the use of such electrolyte for the electropolishing of IN718 fabricated via laser melting PBF-AM. From previous studies it was shown that various process parameters including the electrode spacing, voltage, temperature and polishing time all have significant effects on the surface qualities of the polished samples [29, 30]. It was also suggested that the electrolyte flow could potentially have significant effect on the polishing effect as well due to its influence on the diffusion efficiency of the electrolyte. In this study, the effects of these parameters were investigated for IN718.

Experimentation

The electropolishing station configuration is shown in Fig.1a. The same configuration was also used in previous studies [29, 30]. The glass electropolishing chamber has an inlet and outlet on opposite sides and has a maximum volume of roughly 700mL. The electrical voltage for polishing is controlled by the Instek PSW 160-14.4 power supply, the electrolyte circulation flow is driven by a Masterflex 7523-40 L/S peristaltic pump. A Graham condenser is connected into the electrolyte flow circulation as the heat exchanger for the cooling of the electrolyte, and the cooling bath is provided by a large water tank with temperature control. From previous experiments it was realized that the cooling rate with the use of Graham condenser is limited especially when the flow rate is high. Therefore, in the current study over-compensated control scenario was used, which involved the use of ice water for more rapid cooling once the electropolishing reaction initiated. The sample design is shown in Fig.1b. The thickness of the sample is 1mm, although this dimension is considered less relevant to the current study. The samples were fabricated by a Concept Laser M1 system. The orientation of the sample during the fabrication is also shown in Fig.1b. Therefore, the surfaces used for experimentation are vertical surfaces.



a. Experimental setup

b. Sample design

Fig.1 Electropolishing experimentation configuration

From both previous experiments and the preliminary fluid flow simulation it was shown that the inlet and outlet configuration of the polishing chamber does not introduce well-regulated fluid flow. In order to evaluate the effect of fluid flow, a more regulated laminar flow must be introduced. Therefore, a flow-splitter was introduced in the experimental setup. As shown in Fig.2, the splitter was placed in the polishing chamber near the flow inlet, and the surface of the splitter is aligned with the sample surfaces. In order to verify the effectiveness of the split configuration, additional fluid flow simulations were carried out.

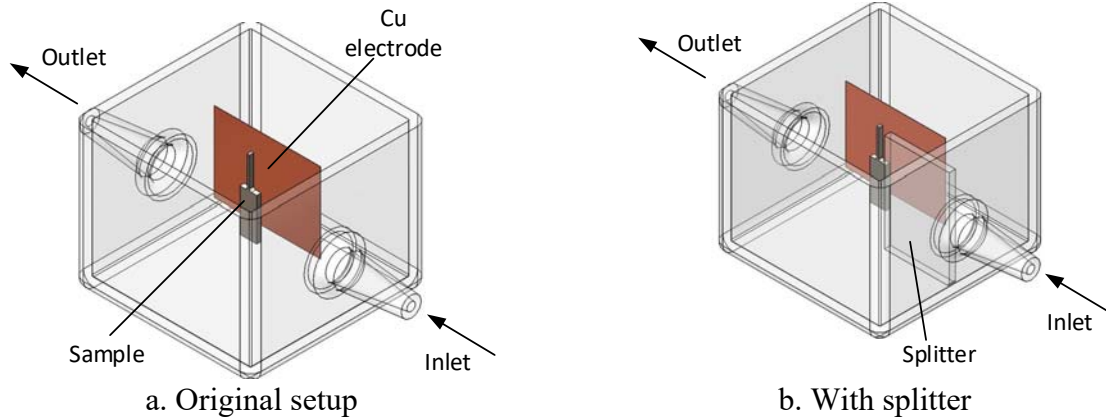


Fig.2 Flow control regulation

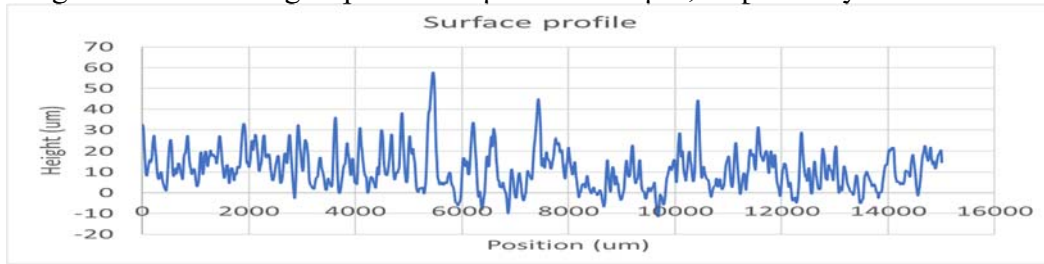
To investigate the effect of each parameter on the surface quality of the IN718 parts, a 5^2 full factorial experimental design was developed. As shown in Table 1, five input variables, including temperature, electrode spacing, voltage, flow rate and split configuration were investigated, with each variables having 2 levels. For the electrolyte, the following recipe was used: 1L of electrolyte should consist of: 700mL of ethyl alcohol, 300mL of isopropyl alcohol, 60g $AlCl_3$ and 250g $ZnCl_2$ [31]. 1 sample was polished for each parameter combinations. After polishing, the surface roughness of the samples were measured with a Dektak 8 profilometer along the longest direction (i.e. build direction as shown in Fig.1b). Three measurements were made for each sample with even spacing across the width of the sample approximated by the eyeballing of the operator. In addition, the surface roughness of the as-received samples was also characterized. In order to verify the effectiveness of the split configuration, additional fluid flow simulations were carried out using SolidWorks Flow Simulation with the flow rate setup shown in Table 1. In the fluid flow simulations, the viscosity value of the electrolyte was taken as 9.58cP, which was obtained via the measurement with the fresh electrolyte solution using viscometer. The effect of temperature on viscosity was ignored during the simulation. The measured surface roughness of the as-received sample was used to set up surface roughness in the simulations. The electrode spacing was set to be 7mm for all the simulations.

Variables	Levels
Temperature ($^{\circ}C/^{\circ}F$)	26.7/80, 37.8/100
Electrode spacing (mm)	7.5, 15
Flow rate (mL/min)	800, 1200
Voltage (V)	60, 80
Split configuration	Yes, No

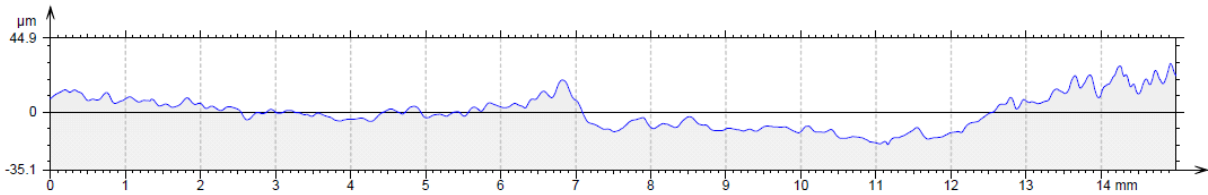
Table 1 Experimental design table

Results and Discussions

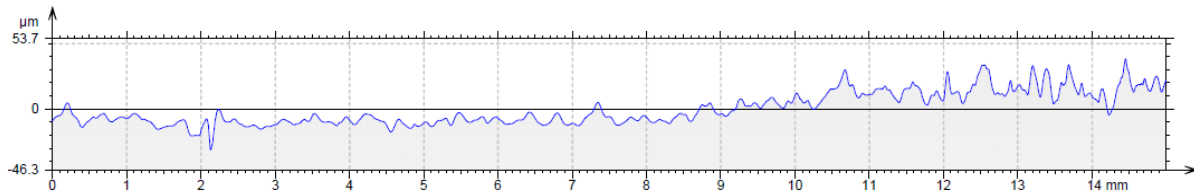
The typical surface profile of the as-received IN718 samples is shown in Fig.3a, while the typical surface profiles of the polished samples are shown in Fig.3b-c. The surface roughness of the as-received samples is $R_a 7.90 \pm 0.326 \mu\text{m}$. It can be observed visually that the surface polish had significant effects, as there exist significantly fewer peaks and valleys on the profiles. The surface roughness R_a of each type of sample are listed in Table 2. The differences between the non-split configuration and split configuration does not appear to be significant, as the average surface roughness of the two groups are $3.05\mu\text{m}$ and $2.98\mu\text{m}$, respectively.



a. As-received



b. 60V-80F-15mm-800mL/m-No splitter



c. 60V-80F-15mm-800mL/m-Splitter

Fig.3 surface profile of the samples

#	Vol (V)	Temp (F)	S (mm)	FR (mL/m)	Split	R_a (μm)	#	Vol (V)	Temp (F)	S (mm)	FR (mL/m)	Split	R_a (μm)
1	60	80	7	800	N	2.678	17	80	80	7	800	N	2.716
2	60	80	7	800	Y	2.728	18	80	80	7	800	Y	4.249
3	60	80	7	1200	N	4.160	19	80	80	7	1200	N	2.682
4	60	80	7	1200	Y	3.123	20	80	80	7	1200	Y	2.991
5	60	80	15	800	N	3.015	21	80	80	15	800	N	3.079
6	60	80	15	800	Y	2.970	22	80	80	15	800	Y	3.762
7	60	80	15	1200	N	2.863	23	80	80	15	1200	N	3.050
8	60	80	15	1200	Y	3.578	24	80	80	15	1200	Y	3.140
9	60	100	7	800	N	1.904	25	80	100	7	800	N	2.080
10	60	100	7	800	Y	2.070	26	80	100	7	800	Y	4.673
11	60	100	7	1200	N	3.003	27	80	100	7	1200	N	4.272
12	60	100	7	1200	Y	2.810	28	80	100	7	1200	Y	2.808
13	60	100	15	800	N	3.297	29	80	100	15	800	N	3.812
14	60	100	15	800	Y	1.808	31	80	100	15	800	Y	2.064
15	60	100	15	1200	N	3.620	31	80	100	15	1200	N	2.512
16	60	100	15	1200	Y	3.112	32		100	15	1200	Y	1.791

Table 2 Surface roughness measurement results

Further analysis with the results using ANOVA provided additional insights into the significance of each design factors and their interactions. Fig.4 shows the standardized effects of design factors on the average surface roughness value of each types of sample. From Fig.4 the 2-way interaction of voltage and flow rate (AD) and the 3-way interaction of electrode spacing (gap), flow rate and split configuration (CDE) both have significant effect on the average surface roughness. From the principles of electropolishing the significance of the 3-way interaction (CDE) is readily justified. During the electropolishing processes the Ni^{2+} ions are released from the samples under the driving energy of the electrical fields, and consequently transported away from the surface via electrolyte circulation. Therefore, the fluid flow characteristics of the electrolyte could significantly influence the mass transportation of the Ni^{2+} ions and consequently the polishing efficiency. This is further elaborated by the results from the fluid flow simulation studies. As shown in Fig.5, for the no-splitter configurations, the fluid flows of the electrolyte exhibit experience significant disruptions at the sample front caused by the sample leading edges, and such effect is more pronounced as the flow rate increases. The fluctuation of the fluid flow rates across the samples are further elucidated in Fig.6, which shows the average fluid flow velocities and their variabilities on the planes parallel to the sample surfaces at varying distances. Without the use of the split configuration, the highest average flow rates of the electrolyte occur at about 1.5mm from the sample surfaces, although the standard deviations also peak at that distance, indicating highly non-uniform electrolyte flow rate. With the split configuration, the maximum average flow rates occur at slightly higher planes (~2mm) from the sample surfaces. Also the variabilities of the average flow rate at difference distances from the sample surfaces as well as the flow rate on each investigated planes are significantly smaller compared to the no-split configurations.

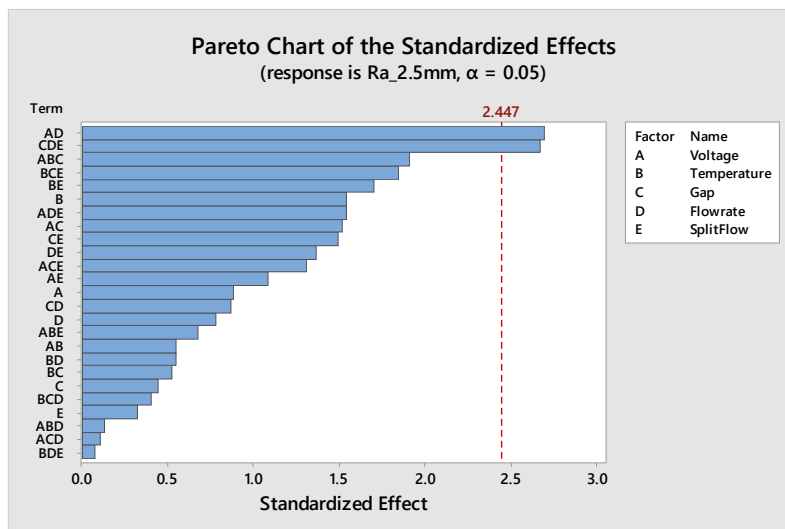
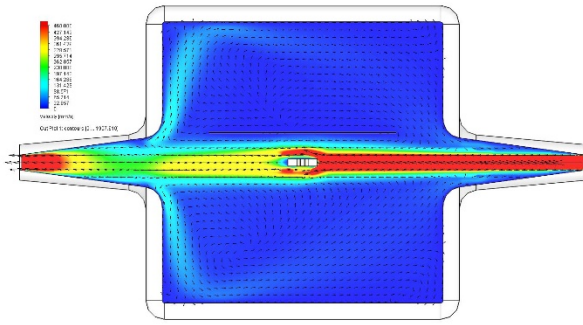
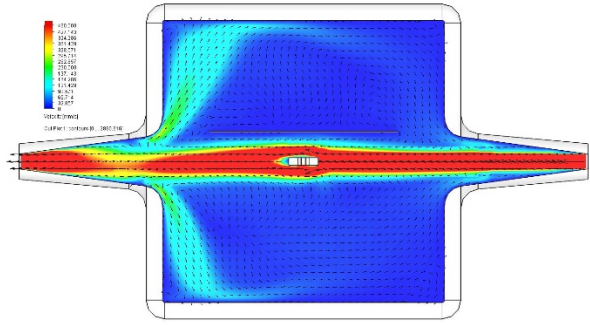


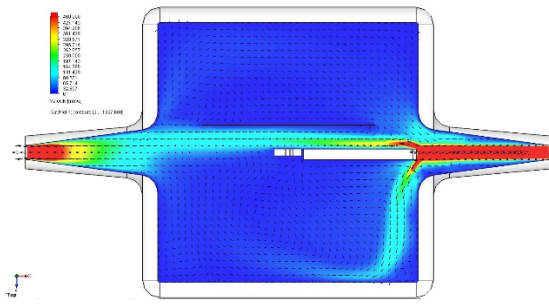
Fig.4 Significance of design factors on average surface roughness



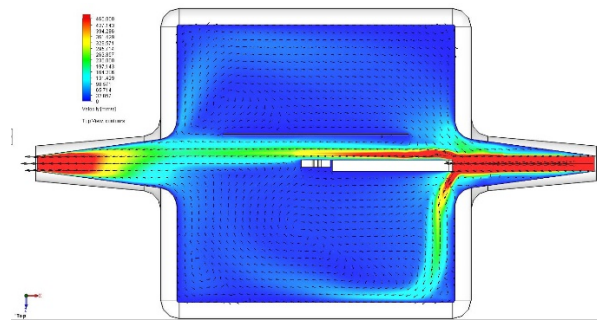
a. 800mL/m flow rate – no split



b. 1200mL/m flow rate – no split

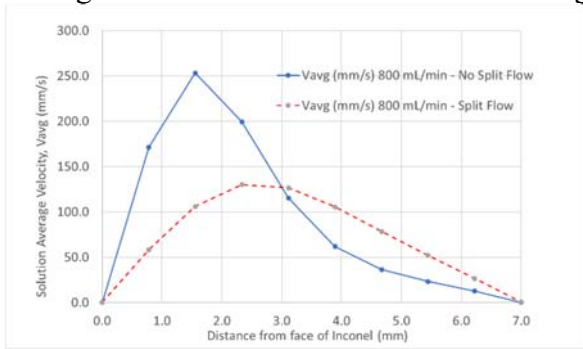


c. 800mL/m flow rate – split

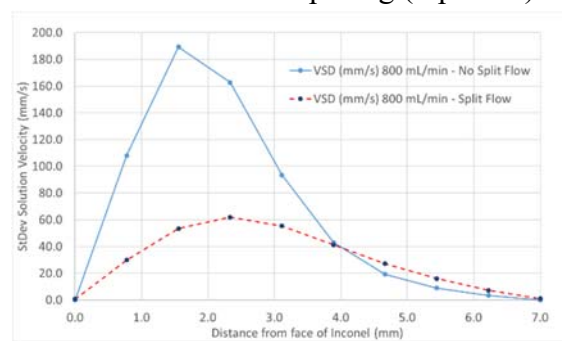


d. 1200mL/m flow rate – split

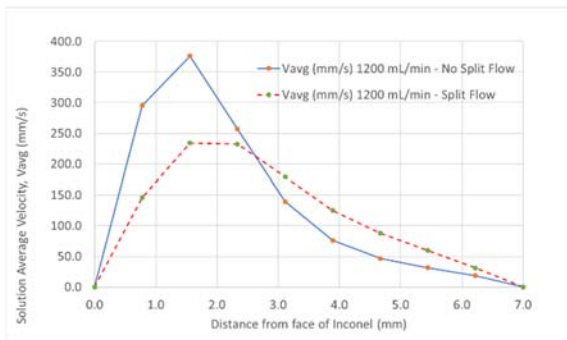
Fig.5 Fluid flow simulations of test configurations – 7mm electrode spacing (top view)



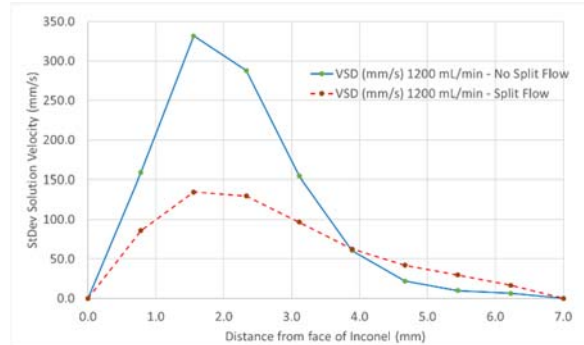
a. 800mL/min average flow velocity



b. 800mL/min flow velocity standard deviation



a. 1200mL/min average flow velocity



b. 1200mL/min flow velocity standard deviation

Fig.6 Flow velocity along the planes at varying distances from the sample surfaces

The better-regulated electrolyte flow control with the split configuration also appears to have some effects on the uniformity of the surface roughness, although the effect is not as significant. Fig.7 shows the standardized effect of design factors on the standard deviation of the surface roughness values. The 3-way interaction of voltage, spacing and flow rate, the temperature, the 2-way interactions of spacing and split configuration as well as voltage and spacing appear to be the most significant factors, although none achieved a significance level that corresponds to a $p < 0.05$ of confidence level.

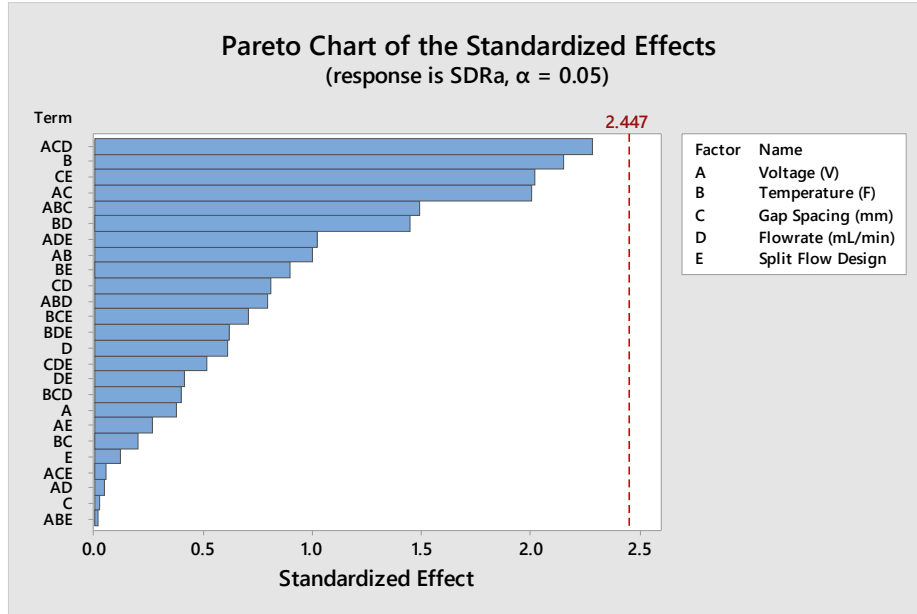


Fig.7 Significance of design factors on surface roughness variabilities

The significance of the interaction between the voltage and the factors for flow control (flow rate, split configuration) might be a result of the change of significance of the ion mass transportation through the electrolyte due to the reaction rate change. With higher electropolishing voltage the ion release rate from the sample might be enhanced, which would facilitate the mass transportation limiting electropolishing mechanism that is highly influenced by the electrolyte flow [32]. On the other hand, the relatively low significance levels for various factors might be a result of the fact that relatively low electropolishing rates were observed in the experiments, which might correspond to a more “passive” electropolishing process that is dominated by macromachining [33]. This electropolishing mechanism tends to be less sensitive to the electrolyte flow and would reduce large features more effectively while lacks the efficiency to reduce micro-protrusions on the part surfaces. In addition, the lack of accurate control of temperature (i.e. via the use of ice-water that establishes an open-loop control) might also have contributed to the low significance of temperature factor despite the previous experimental observations with Ti6Al4V [29, 30].

Conclusions

In this study, an experimental design was employed to evaluate the significance of various process variables (voltage, temperature, electrode spacing, electrolyte flow rate and flow rate uniformity) on the surface quality of the IN718 parts fabricated via laser melting PBF-AM process. Overall the use of electropolishing was able to achieve average surface roughness of $R_a \sim 3\mu\text{m}$ that is a significant improvement compared to the original surfaces. The voltage used for the experiment might not have achieved a significant level to introduce mass transportation limiting

polishing mechanism. Therefore, although more regulated electrolyte flow appear to have effects on the surface finish quality, such effect is not as significant as originally expected. The use of splitter for the control of electrolyte flow appears to be an effective method for such purpose, which can be utilized in the future for continuous research of this subject.

Acknowledgement

The authors are grateful for the support of this work by NASA Marshall Space Flight Center Contract #SC-2019-004 and NASA Kentucky EPSCoR Grant RID-3 #7800003125. The authors would also like to acknowledge the support of Rapid Prototyping Center (RPC) and Conn Center of Renewable Energy at University of Louisville.

References

- [1] A. Thomas, M. El-Wahabi, J. M. Cabrera, J. M. Prado. High temperature deformation of Inconel 718. *Journal of Materials Processing Technology*. 177(2006): 469-472.
- [2] M. Rahman, W. K. H. Seah, T. T. Teo. The machinability of Inconel 718. *Journal of Materials Processing Technology*. 63(1997): 199-204.
- [3] S. Azadian, L.-Y. Wei, R. Warren. Delta phase precipitation in Inconel 718. *Materials Characterization*. 53(2004): 7-16.
- [4] M. Anderson, R. Patwa, Y. C. Shin. Laser-assisted machining of Inconel 718 with an economic analysis. *International Journal of Machine Tools & Manufacture*. 46(2006): 1879-1891.
- [5] X. Han, L. Wu, H. Xia, R. Liu, S. Wang, Z. Chen. Superplastic properties of Inconel 718. *Journal of Materials Processing Technology*. 137(2003): 17-20.
- [6] G. A. Rao, M. Kumar, M. Srinivas, D. S. Sarma. Effect of standard heat treatment on the microstructure and mechanical properties of hot isostatically pressed superalloy inconel 718. *Materials Science and Engineering A*. 355(2003): 114-125.
- [7] J. M. Pereira, B. A. Lerch. Effects of heat treatment on the ballistic impact properties of Inconel 718 for jet engine fan containment applications. *International Journal of Impact Engineering*. 25(2001): 715-733.
- [8] D. G. Thakur, B. Ramamoorthy, L. Vijayaraghavan. Machinability investigation of Inconel 718 in high-speed turning. *International Journal of Manufacturing Technologies*. 45(2009): 421-429.
- [9] D. Dudzinski, A. Devillez, A. Moufki, D. Larrouquere, V. Zerrouki, J. Vigneau. A review of developments towards dry and high speed machining of Inconel 718 alloy. *International Journal of Machine Tools and Manufacture*. 44(2004): 439-456.
- [10] H. R. Krain, A. R. C. Sharman, K. Ridgway. Optimisation of tool life and productivity when end milling Inconel 718TM. *Journal of Materials Processing Technology*. 189(2007): 153-161.
- [11] Q. Jia, D. Gu. Selective laser melting additive manufacturing of Inconel 718 superalloy parts: densification, microstructure and properties. *Journal of Alloys and Compounds*. 585(2014): 713-721.
- [12] K. N. Amato, S. M. Gaytan, L. E. Murr, E. Martinez, P. W. Shindo, J. Hernandez, S. Collins, F. Medina. Microstructures and mechanical behavior of Inconel 718 fabricated by selective laser melting. *Acta Materialia*. 60(2012): 2229-2239.
- [13] Q. Jia, D. Gu. Selective laser melting additive manufactured Inconel 718 superalloy parts: high-temperature oxidation property and its mechanisms. *Optics and Laser Technology*. 62(2014): 161-171.

- [14] Z. Wang, K. Guan, M. Gao, X. Li, X. Chen, X. Zeng. The microstructure and mechanical properties of deposited-IN718 by selective laser melting. *Journal of Alloys and Compounds*. 513(2012): 518-523.
- [15] G. Strano, L. Hao, R. M. Everson, K. E. Evans. Surface roughness analysis, modelling and prediction in selective laser melting. *Journal of Materials Processing Technology*. 213(2013): 589-597.
- [16] K. Mumtaz, N. Hopkinson. Top surface and side roughness of Inconel 625 parts processed using selective laser melting. *Rapid Prototyping Journal*. 15(2009), 2: 96-103.
- [17] E. Yasa, J.-P. Kruth, J. Deckers. Manufacturing by combining selective laser melting and selective laser erosion/laser re-melting. *CIRP Annuals- Manufacturing Technology*. 60(2011): 263-266.
- [18] A. Bauereiss, T. Scharowsky, C. Korner. Defect generation and propagation mechanism during additive manufacturing by selective beam melting. *Journal of Materials Processing Technology*. 214(2014): 2522-2528.
- [19] S. Ly, A. M. Rubenchik, S. A. Khairallah, G. Guss, M. J. Matthews. Metal vapor micro-jet controls material redistribution in laser powder bed fusion additive manufacturing. *Scientific Reports*. 7(2017): 4085.
- [20] E. Yasa, J. Deckers, J.-P. Kruth. The investigation of the influence of laser re-melting on density, surface quality and microstructure of selective laser melting parts. *Rapid Prototyping Journal*. 17(2011), 5: 312-327.
- [21] C. A. Huang, T. H. Wang, W. C. Han, C. H. Lee. A study of the galvanic corrosion behavior of Inconel 718 after electron beam welding. *Materials Chemistry and Physics*. 104(2007): 293-300.
- [22] M. Turner, G. E. Thompson, P. A. Brook. The anodic behaviour of nickel in sulphuric acid solution. *Corrosion Science*. 13(1973), 12: 985-990.
- [23] S. Kissling, K. Bade. Electrochemical finishing of nickel microstructures. In *Multi-Material Micro Manufacture*. Edited by S. Dimov, W. Menz. Whittles Publishing Ltd. 2008.
- [24] C. A. Huang, Y. C. Chen, J. H. Chang. The electrochemical polishing behavior of the Inconel 718 alloy in perchloric-acetic mixed acids. *Corrosion Science*. 50(2008): 480-490.
- [25] W. Simka, M. Kaczmarek, A. Baron-Wiechec, G. Nawrat, J. Marciniak, J. Zak. Electropolishing and passivation of NiTi shape memory alloy. *Electrochimica Acta*. 55(2010): 2437-2441.
- [26] K. Fushimi, M. Stratmann, A. W. Hassel. Electropolishing of NiTi shape memory alloys in methanolic H₂SO₄. *Electrochimica Acta*. 52(2006): 1290-1295.
- [27] A. Kuhn. The electropolishing of titanium and its alloys. *Metal Finishing*. 102(2004), 6: 80-86.
- [28] C. A. Huang, F.-Y. Hsu, C. H. Yu. Electropolishing behavior of pure titanium in sulfuric acid-ethanol electrolytes with an addition of water. *Corrosion Science*. 53(2011): 589-596.
- [29] L. Yang, A. Lassell, G. P. V. Paiva. Further study of the electropolishing of Ti6Al4V parts made via electron beam melting. *Proceedings of the International Solid Freeform Fabrication (SFF) Symposium, Austin, TX, 2015*.
- [30] L. Yang, Y. WU, A. Lassell, B. Zhou. Electropolishing of Ti6Al4V parts fabricated by electron beam melting. *Proceedings of the International Solid Freeform Fabrication (SFF) Symposium, Austin, TX, 2016*.

- [31] K. Tajima, M. Hironaka, K.-K. Chen, Y. Nagamatsu, H. Kakigawa, Y. Kozono. Electropolishing of CP titanium and its alloys in an alcoholic solution-based electrolyte. *Dental Materials Journal*. 27(2008), 2: 258-265.
- [32] D. Landolt, P.-F. Chauvy, O. Zinger. Electrochemical micromachining, polishing and surface structuring of metals: fundamental aspects and new developments. *Electrochimica Acta*. 48(2003): 3185-3201.
- [33] D. Landolt. Fundamental aspects of electropolishing. *Electrochimica Acta*. 32(1987), 1:1-11.